

# Fragmentation path of excited nuclear systems

M. Colonna<sup>a</sup>, G. Fabbri<sup>b</sup>, M. Di Toro<sup>a</sup>, F. Matera<sup>b</sup>,  
H.H. Wolter<sup>c</sup>

<sup>a</sup>*Laboratori Nazionali del Sud, Via S. Sofia 44, I-95123 Catania,  
and Physics-Astronomy Dept., University of Catania, Italy*

<sup>b</sup>*Dipartimento di Fisica, Universita' di Firenze, and INFN, Sez. di Firenze, Italy*

<sup>c</sup>*Sektion Physik, Universitat Muenchen, Garching, Germany*

---

## Abstract

We perform a study of the fragmentation path of excited nuclear sources, within the framework of a stochastic mean-field approach. We consider the reaction  $^{129}\text{Xe} + ^{119}\text{Sn}$  at two beam energies: 32 and 50 MeV/A, for central collisions. It is observed that, after the compression phase the system expands towards a dilute configuration from which it may recontract or evolve into a bubble-like structure. Then fragments are formed through the development of volume and/or surface instabilities. The two possibilities co-exist at 32 MeV/A, leading to quite different fragment partitions, while at 50 MeV/A the hollow configuration is observed in all events. Large variances are recovered in a way fully consistent with the presence of spinodal decomposition remnants. Kinematical properties of fragments are discussed and suggested as observables very sensitive to the dominant fragment production mechanism. A larger radial collective flow is observed at 50 MeV/A, in agreement with experiments.

*Key words:* Multifragmentation; Low-density instabilities; Stochastic approaches; Dynamical description of fragmentation path; Central collisions.

PACS numbers: 21.30.Fe, 25.70.-z, 25.70.Lm, 25.70.Pq.

---

## 1 Introduction

The observation of several intermediate mass fragments (IMF) in heavy ion collisions and the possible connection to the occurrence of liquid-gas phase transitions in nuclear systems are still among the most challenging problems in heavy ion reaction physics.

Recently many efforts have been devoted to identify relevant observables that may signal the occurrence of phase transitions in finite nuclei [1–5]. These studies are mostly based on the investigation of thermodynamical properties of finite systems at equilibrium and on critical behaviour analyses. In such a context, a description of the dynamics of fragment formation can provide an important complementary piece of information to learn about the path of the fragmentation process. Indeed the study of the dynamical evolution of complex excited nuclear systems may shed some light on the relevant fragmentation mechanisms and on density and temperature conditions where fragments are formed. This opens the possibility to get insight into the behaviour of the system in such regions, far from normal values, encountered along the fragmentation path, and hence on its equation of state (EOS). Eventually at the freeze-out configuration one may check how the available phase space has been filled and compare results obtained for some relevant degrees of freedom and physical observables to the values expected at thermodynamical equilibrium. At the same time one may try to identify some specific observables that keep the memory of the fragmentation mechanism and are sensitive to the EOS.

In this article we present an analysis of the fragmentation dynamics of excited nuclear sources that are formed in central heavy ion collisions at intermediate energies. This study is performed within the framework of stochastic mean field approaches [6–9]. As extensively discussed also in Ref.[10], according to this theory, the fragmentation process is dominated by the growth of volume (spinodal) and surface instabilities encountered during the expansion phase of the considered excited systems. Hence the fragmentation path is driven by the amplification of the unstable collective modes. The correct description of the degree of thermal agitation, that determines the amplitude of the stochastic term incorporated in the treatment, is essential since fluctuations provide the seeds of fragment formation.

We notice here that this scenario for fragment formation occurs in several many-body systems. Indeed spinodal instabilities have been shown to drive the fragmentation path of dilute classical systems of particles interacting through short-range forces, for which exact dynamical calculations can be performed [11–13], and are a well known mechanism in the decomposition of binary alloys [14]. The role of spinodal instabilities in nuclear fragmentation has been recently investigated also in experimental data [15,5].

Multifragmentation studies have been undertaken also in the framework of molecular dynamics approaches for fermions [16–18]. It would be interesting to investigate whether, according to these models, fragments appear already in the high-density phase, due to the presence of strong N-body correlations, or a composite almost uniform system may survive until it enters low density regions, as it happens within our scenario. In the two cases fragment formation would be sensitive to different regions of the nuclear EOS and one expects to

see differences especially in charge and velocity correlations and in the isotopic content.

In this article, calculations are performed using the stochastic mean-field method described in Ref.[8]. With respect to previous studies, the method employed here has a larger domain of applicability. Indeed we implement density fluctuations locally in coordinate space to mimic the effect of the local thermal equilibrium fluctuations. This can be done at each time and in each configuration, the only requirement being the condition of local thermal equilibrium. On the other hand, in the approaches used in previous works [7], a stochastic force was introduced, whose strength can be tuned to reproduce the correct fluctuation amplitude of few fragmentation modes, thus requiring the knowledge of the most important ones.

Moreover, the method of Ref.[8] can be easily extended to fragmentation studies of charge asymmetric systems [19], of large interest nowadays. In fact fluctuations can be implemented separately for protons and neutrons, on the basis of their respective kinetic equilibrium fluctuations.

We perform calculations for systems of experimental interest, showing how physical observables can be related to the degree and the kind of instability encountered.

The paper is organized as follows: In Section 2 we recall the main features of the method, describing in more detail the procedure to inject fluctuations; In Section 3 results on the fragmentation dynamics of excited nuclear sources are presented. Some conclusions are drawn in Section 4.

## 2 Description of the method

Theoretically the evolution of complex systems under the influence of fluctuations can be described by a transport equation with a stochastic fluctuating term, the so-called Boltzmann-Langevin equation (BLE):

$$\frac{df}{dt} = \frac{\partial f}{\partial t} + \{f, H\} = I_{coll}[f] + \delta I[f], \quad (1)$$

where  $f(\mathbf{r}, \mathbf{p}, t)$  is the one-body distribution function,  $H(\mathbf{r}, \mathbf{p}, t)$  is the one-body Hamiltonian and  $\delta I[f]$  represents the stochastic part of the two-body collision integral [20,21]. Exact numerical solutions of the BLE are very difficult to be obtained and they have only been calculated for schematic models in two dimensions [22]. Therefore various approximate treatments of the BLE have been introduced [23,7,8]. In the Brownian One Body (BOB) dynam-

ics, developed in Ref.[7], the fluctuating part of the collision integral  $\delta I$  is replaced by a stochastic force added to the standard Boltzmann-Nordheim-Vlasov (BNV) equation (i.e. Eq.(1) without stochastic term), the strength of which can be tuned to correctly describe the growth of the most important unstable modes.

Here we will follow the method introduced in Ref.[8].

Within the assumption of local thermal equilibrium, the stochastic term of Eq.(1) essentially builds the kinetic equilibrium fluctuations typical of a Fermi gas:  $\sigma_f^2 = f(1 - f)$ , where  $f(\mathbf{r}, \mathbf{p}, t)$  can be approximated by a Fermi-Dirac distribution,  $f(\mathbf{r}, \mathbf{p}, t) = 1/(1 + e^{(\epsilon - \mu)/T})$  with local chemical potential and temperature,  $\mu(\mathbf{r}, t)$ ,  $T(\mathbf{r}, t)$ . We project on density fluctuations obtaining:

$$\sigma_{\rho,eq}^2(\mathbf{r}, t) = \frac{1}{V} \int \frac{d\mathbf{p}}{h^3/4} \sigma_f^2(\mathbf{r}, \mathbf{p}, t) = \frac{T}{V} \frac{3\rho}{2\epsilon_F} \left(1 - \frac{\pi^2}{12} \left(\frac{T}{\epsilon_F}\right)^2 + \dots\right), \quad (2)$$

where we have used the Sommerfeld expansion around  $\epsilon = \mu$  for small  $T/\epsilon_F$  ( $\epsilon_F$  denotes the Fermi energy).

Actually this kinetic equilibrium value is reached asymptotically for an ideal gas of fermions. After a small time step  $\Delta t$ , the value reached for the density fluctuations can be approximated by:

$$\sigma_{\rho}^2(\mathbf{r}, t, \Delta t) = \sigma_{\rho,eq}^2(\mathbf{r}, t) \frac{2\Delta t}{\tau_{coll}(\mathbf{r}, t)}, \quad (3)$$

where  $\tau_{coll}$  is the damping time associated with the two-body collision process. At temperatures around 4 MeV, that are typically reached in fragmentation processes,  $\tau_{coll}$  is of the order of 50 fm/c [24]. In our calculations fluctuations are injected each  $\Delta t = 5$  fm/c and their amplitude is scaled accordingly (see Eq.(3)). In the cell of  $\mathbf{r}$  space being considered, the density fluctuation  $\delta\rho$  is selected randomly according to the gaussian distribution  $exp(-\delta\rho^2/2\sigma_{\rho}^2)$ . This determines the variation of the number of particles contained in the cell. A few left-over particles are randomly distributed again to ensure the conservation of mass. Momenta of all particles are finally slightly shifted to ensure momentum and energy conservation.

The fluctuations introduced are then amplified by the unstable mean-field. It is important to notice that the characteristic growth time for the unstable modes is smaller ( $\tau \approx 30$  fm/c) [10] than the collisional damping time, so two-body collisions act just as a seed to perturb the density profile of the system, but the dynamics is essentially driven by the propagation of the mean-field instabilities.

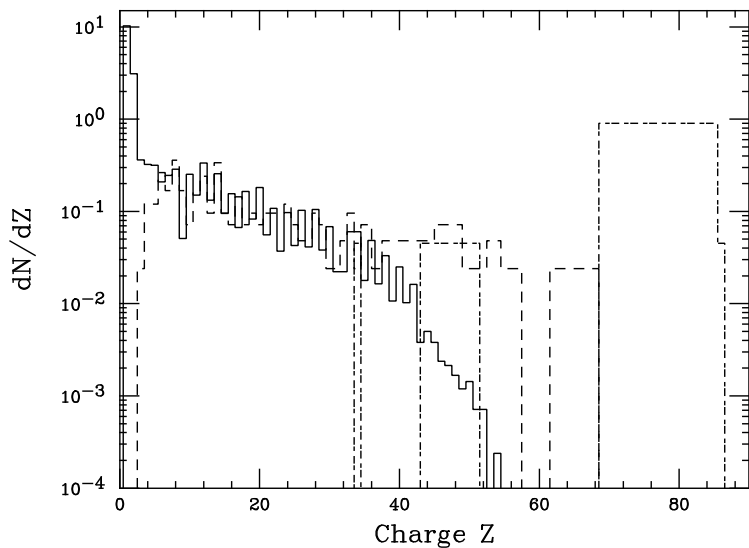


Fig. 1. Primary charge distribution obtained for the nuclear source:  $A = 247$ ,  $Z = 103$ ,  $T = 8.3$  MeV,  $R = 6.6$  fm,  $\beta = 0.09$   $r/R$ , with (long-dashed histogram) and without (short-dashed histogram) including fluctuations. The full histogram represents the final charge distributions obtained in the case including fluctuations.

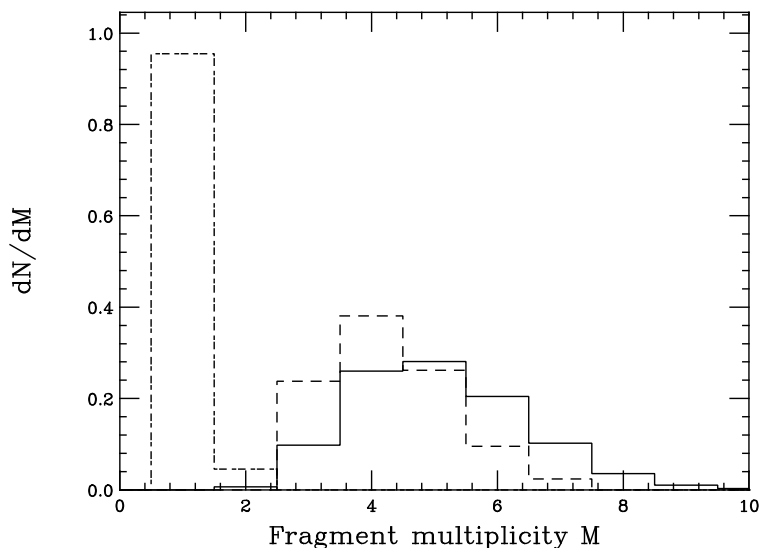


Fig. 2. Fragment multiplicity distribution obtained for the same case as in Fig.1. Symbols are as in Fig.1.

### 3 Presentation of the results and discussion

In order to investigate the fragmentation path followed by excited dilute sources, we start considering a spherical system of radius  $R = 6.6$  fm con-

taining  $A = 247$  nucleons and  $Z = 103$  protons.  $T = 8.3$  MeV is the initial temperature and the system undergoes a self-similar expansion with velocity  $\beta(r) = v(r)/c = 0.09 r/R$ . These properties correspond to the composite source formed in the reaction  $^{129}\text{Xe} + ^{119}\text{Sn}$  at 32 MeV/A, at zero impact parameter, just after the maximum compression has been reached, according to deterministic BNV calculations (no fluctuations included). For the same system calculations have been performed also using the BOB treatment [7].

We use the test particle method, with 200 test particles per nucleon. This ensures a quite good mapping of the phase space, since each test particle is associated with a triangular function of width  $\approx 1$  fm [6]. We adopt a Skyrme-like parameterization of the mean-field potential, corresponding to a soft EOS (compressibility modulus  $K = 200$  MeV).

The dynamical evolution of the system is followed until 240 fm/c. Fluctuations are introduced since the beginning, then they are already present when the system encounters instabilities.

To underline the important role of fluctuations in the dynamical evolution of the system, we also perform simulations turning off fluctuations, i.e. following the standard BNV dynamics. In this case, the initial spherical symmetry and uniform radial distribution are so well preserved that the system, after a moderate expansion, eventually recontracts and does not fragment while in the full treatment (including fluctuations) fragmentation is observed.

In Fig.1 we show the charge distribution obtained at the end of the dynamical simulations, with (long-dashed histogram) and without (short-dashed histogram) fluctuations. The final charge distribution, obtained after secondary de-excitation has been taken into account [25], is shown for the simulations including fluctuations (full histogram). We remark that the final charge distribution is in good agreement with the results obtained with the BOB method [7] and with experimental data [26].

It is clear that in the case without fluctuations the system essentially recontracts, as signaled by the peak at very large  $Z$ . This is evident also from the fragment ( $Z \geq 3$ ) multiplicity distribution (Fig.2). On the other hand, in the calculations including fluctuations the system breaks up into 5 fragments, on average.

In fig.3 we show the average kinetic energy, as a function of the fragment charge, obtained for primary (dashed histogram) and final (full histogram) fragments. The fragment velocities are essentially due to the (low) radial collective flow, related to the expansion of the system, and to the Coulomb repulsion. The latter is responsible of the large difference observed between primary and final kinetic energies. Indeed at the freeze-out configuration the Coulomb repulsion is still important.

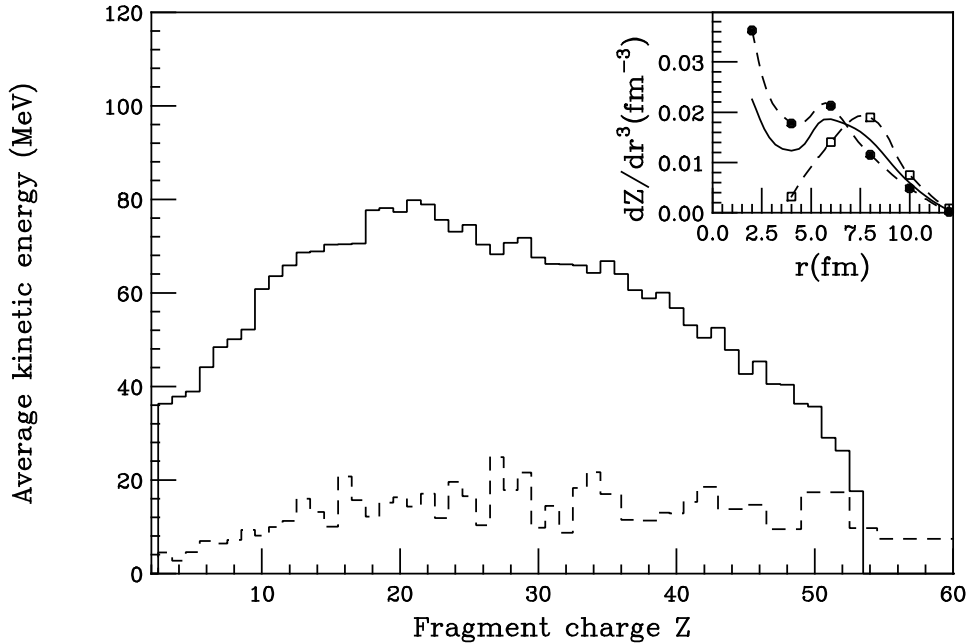


Fig. 3. Average kinetic energies for primary (dashed histogram) and final (full histogram) fragments obtained in the same case as in Figs 1,2. In the inset we show the fragment charge density as a function of the radial distance  $r$  (full line). The results obtained considering only multiplicities  $M=3,4$  (full circles) and  $M=5,6,7$  (squares) are also displayed.

The structure of the freeze-out configuration is illustrated in the inset, where we plot the charge density as a function of the distance from the center of mass of the system,  $r$  (full line). It is possible to observe that, on average, the charge of the fragmenting system is located close to the center of mass and at a distance  $r \approx 7 \text{ fm}$ , where a second bump is observed. This interesting behaviour is due to the fact that, when fluctuations are introduced, the system may recontract in some cases, leading to the formation of fragments close to the center of mass, or develop into a bubble-like structure. Of course, events where some fragments form close to the center, accompanied by lighter fragments located at larger distance are also observed. From a more detailed analysis, it is possible to see that in events with low IMF multiplicity,  $M_{IMF} = 3, 4$ , the charge is mostly concentrated close to the center of mass (full circles), indicating that more compact configurations with coupled surface and volume instabilities [27] are formed, while in events with larger multiplicity, from 5 to 7, fragments are observed around  $r \approx 8 \text{ fm}$ , at the boundary of a hollow configuration (squares). The growth times of instabilities are different in the two cases, the hollow configuration being more unstable. In fact the system reaches a higher degree of dilution in this situation. Hence two scenarios of fragment formation seem to co-exist, yielding quite different fragment

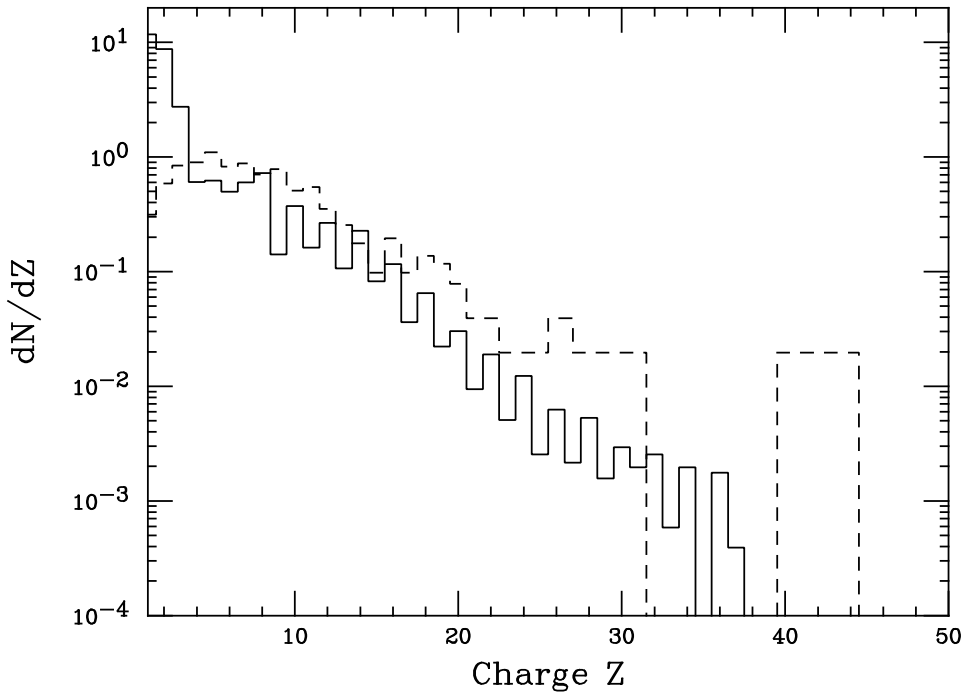


Fig. 4. Charge distribution obtained for the nuclear source:  $A = 244$ ,  $Z = 101$ ,  $T = 10$  MeV,  $R = 7.5$  fm,  $\beta = 0.13 r/R$ , for final (solid histogram) and primary (dashed histogram) fragments.

partitions and a broad charge distribution (see Fig.1). The fact that large IMF's are mostly located close to the center is reflected also in the decreasing behaviour of the average kinetic energy observed at large  $Z$  (see Fig.3).

To appreciate how the fragmentation mechanism evolves with the energy stored in the system, now we turn to consider the dynamical evolution of an excited spherical source with the following properties:  $A = 244$ ,  $Z = 101$ , temperature  $T = 10$  MeV, radius  $R = 7.5$  fm, and with a self similar radial velocity  $\beta = 0.13 r/R$ . This system is obtained in the collision  $^{129}\text{Xe} + ^{119}\text{Sn}$  at 50 MeV/A, at the beginning of the expansion towards densities lower than the normal value.

In this case it is observed that, as a property of the average dynamics, i.e. even without including fluctuations, the nucleus expands into a hollow, quasi stationary configuration, that evolves rather slowly, while, as we have seen before, at lower energies the system essentially recontracts in absence of fluctuations [28].

Actually the spatial geometry of the fragmenting system has been the object of several investigations, within BUU-like approaches [29]. In many cases the formation of a bubble-like structure has been reported. This is due to the



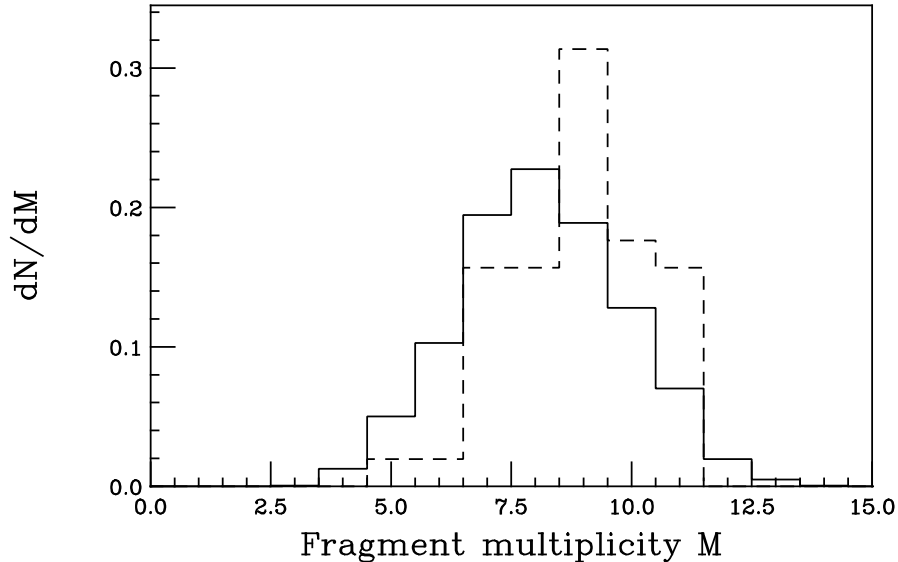


Fig. 5. Multiplicity distribution for the same case as in Fig.4, obtained for final (solid histogram) and primary (dashed histogram) fragments.

competition between the radial expansion flow and the velocity field that develops at the surface. In fact the latter tries to recompact the system.

The hollow configuration is unstable against density fluctuations that break the spherical symmetry. Hence, including self-consistent fluctuations in the dynamics, fragment formation is observed. Fig.4 shows the fragment charge distribution (dashed histogram) obtained at the freeze-out time,  $t = 140 \text{ fm}/c$ . The final charge distribution is also displayed (full histogram).

The system explodes into lighter IMF's, as indicated already by the primary charge distribution. Moreover the number of nucleons and light particles that are emitted while fragments are formed is larger in this reaction, with respect to the case at  $32 \text{ MeV}/A$ . In fact, the total charge of the IMF's ( $Z \geq 3$ ) produced at the freeze-out changes from 84 (at  $32 \text{ MeV}/A$ ) to 75 (at  $50 \text{ MeV}/A$ ).

The IMF multiplicity distribution is presented in Fig.5. It is interesting to notice that the average number of primary IMF's is larger than the final one. This is due to the fact that very light IMF's ( $Z=3$  or  $4$ ) present at the freeze-out configuration may decay into free nucleons and light particles.

The spatial distribution of fragments is illustrated in the inset of Fig.6. Now it is possible to observe that fragments are mostly distributed around  $r = 12 \text{ fm}$ .

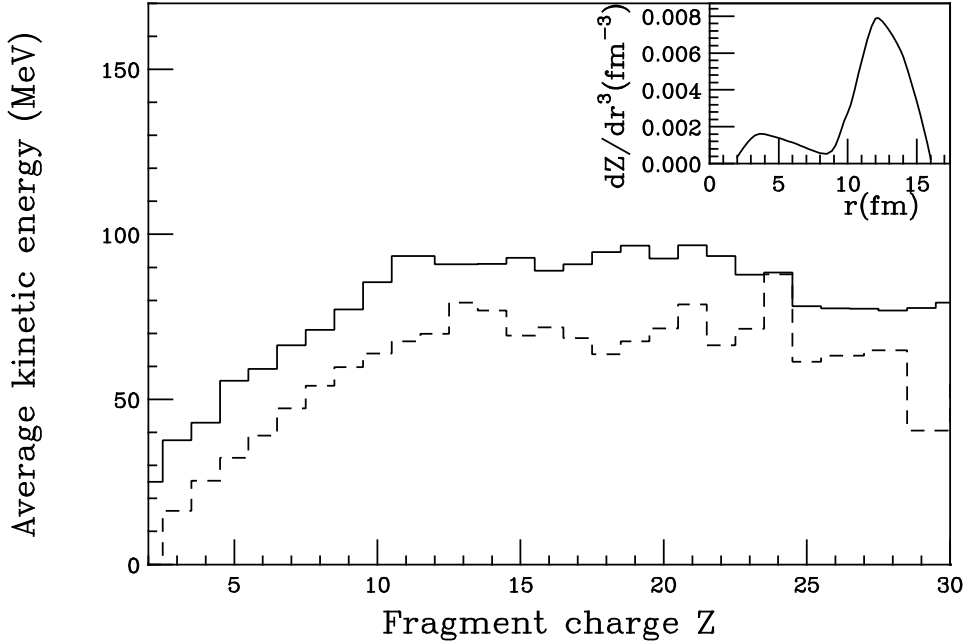


Fig. 6. *Fragment average kinetic energy as obtained in our simulations for primary (dashed histogram) and final (full histogram) fragments. In the inset we show the fragment charge density as a function of the radial distance  $r$ .*

So, with respect to the case at lower energy previously discussed, the bulk of the system appears more concerned by the instabilities and the system breaks up into a larger number of smaller fragments. The average kinetic energy, as a function of the fragment charge, is shown in Fig.6, for primary (dashed histogram) and final fragments (full histogram). Now primary and final kinetic energies are similar since at the freeze-out configuration fragments are already quite well separated and the Coulomb repulsion is small. We notice also the larger radial collective flow obtained in this case.

Finally, in Fig.7 we report the distribution of the largest final fragment,  $Z_{max}$  observed event by event, for the two reactions considered. A broader distribution is obtained at 32 MeV/A, indicating that configurations where large fragments are present co-exist with cases where only light IMF's are formed. On the other hand, large fragments ( $Z > 40$ ) are not observed at 50 MeV/A, fragment partitions are less fluctuating event by event and the  $Z_{max}$  distribution has a smaller width.

We would like to notice that the results reported here are in qualitative agreement with the trend observed in experimental data [26,30]. For the reaction at 32 MeV/A, a careful comparison between data and stochastic calculations performed with BOB can be found in Ref.[26]. For the same reaction the pres-

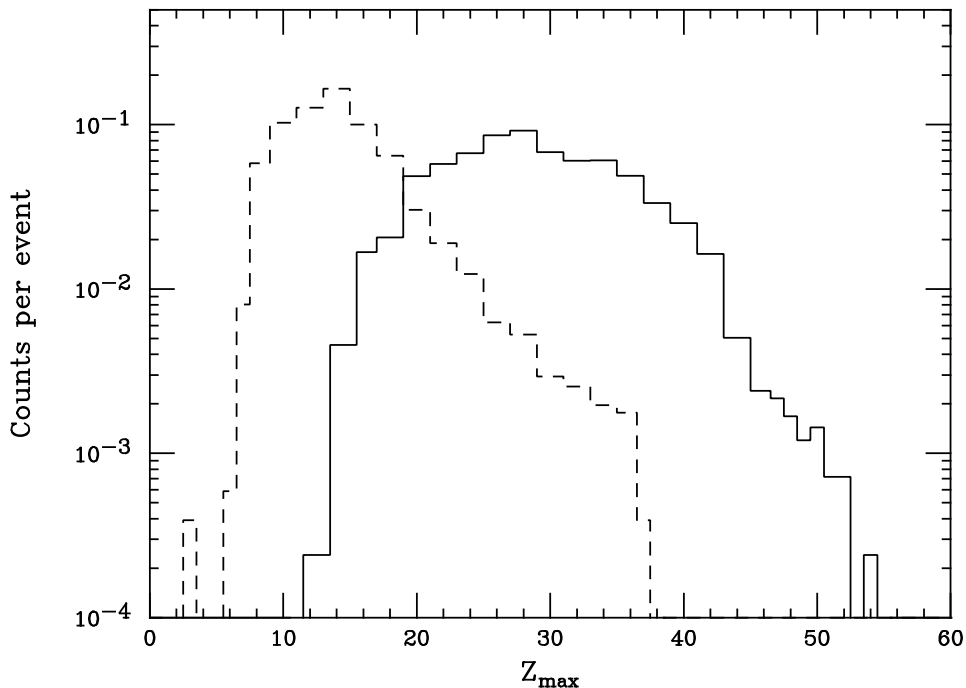


Fig. 7. *Distribution of the largest fragment obtained in the reaction  $^{129}\text{Xe} + ^{119}\text{Sn}$  at 32 MeV/A (full histogram) and 50 MeV/A (dashed histogram).*

ence of spinodal decomposition remnants, i.e. the observation of a few events with nearly equal-sized fragments, has been found in the data, as well as in the simulations [5].

It would be interesting to try to extract information, from the experimental point of view, on the shape of fragment configurations, such as, for instance, the formation of a bubble-like structure that we observe in the simulations at 50 MeV/A. This kind of analysis has been recently undertaken also in light ion induced fragmentation studies [31,32].

## 4 Conclusions

In this article we perform a study of the fragmentation path followed by excited nuclear systems formed in central heavy ion collisions, at two different beam energies. According to stochastic mean-field theories, fragmentation happens during the expansion phase and thus it is related to the properties of the nuclear system at low density and, in particular, to the occurrence of volume and shape instabilities. This opens the possibility to learn about the behaviour of the nuclear EOS at low density.

Mean-field calculations show that, in central heavy ion collisions, the reaction mechanism evolves, with increasing beam energy, from the formation of a single primary source (i.e. incomplete fusion) to fragmentation. In particular, in a given energy range, monopole oscillations push the system towards a metastable configuration, that may recontract, in some cases, or develop into a hollow configuration that eventually fragments. This is what is observed, for the reaction  $^{129}\text{Xe} + ^{119}\text{Sn}$ , at 32 MeV/A. Large fluctuations in the fragment configurations appear in this case, because of the coexistence of the two mechanisms. This is in line with recent experimental observations, that have been related to the occurrence of negative specific heat [33]. The presence of a few events with equal-sized fragments, that may signal the occurrence of spinodal decomposition, has also been reported [5]. At 50 MeV/A the dynamics is dominated by the formation of hollow structures that break up into fragments. A larger collective flow is observed in this case and a larger number of IMF's is formed already at the primary level, together with light particles. In this way we expect to see the transition from the fragmentation regime to vaporization, observed at higher energies.

## References

- [1] R.Botet et al., Phys. Rev. Lett. **86** (2001) 3514; J.D.Frankland et al., contribution to the XLth Int. Wint. Meet. on Nuclear Physics, Bormio (Italy), January 21-25 2002
- [2] J.B.Elliott et al., Phys. Rev. Lett. **88** (2002) 042701
- [3] M.D'Agostino et al., Nucl. Phys. **A699** (2002) 795
- [4] Ph.Chomaz and F.Gulminelli, Nucl. Phys. **A647** (1999) 153; F.Gulminelli, Ph.Chomaz, Al.H.Raduta, Ad.R.Raduta, Phys.Rev.Lett. **91** (2003) 202701
- [5] G.Tabacaru et al., Eur. Phys.J. **A18** (2003) 103
- [6] A.Guarnera, M.Colonna, Ph.Chomaz, Phys. Lett. **B373** (1996) 297
- [7] Ph.Chomaz et al., Phys. Rev. Lett. **73** (1994) 3512; A.Guarnera et al., Phys. Lett. **B403** (1997) 191
- [8] M.Colonna et al., Nucl. Phys. **A642** (1998) 449
- [9] F.Matera, A.Dellafiore, G.Fabbri, Phys. Rev. **C67** (2003) 034608
- [10] Ph.Chomaz, M.Colonna, J.Randrup, Phys. Rep. **389** (2004) 263
- [11] B.Jacquot, A.Guarnera, Ph.Chomaz, M.Colonna, Phys. Lett. **B386** (1996) 23
- [12] S.Pratt, C.Montoya, F.Ronning, Phys. Lett. **B349** (1995) 261
- [13] C.Dorso and J.Randrup, Phys. Lett. **B232** (1989) 29

- [14] J.D.Gunton, M.San Miguel, P.S.Sahni, Phase transitions and Critical Phenomena, Vol.8, Academic Press, New York, 1983.
- [15] B.Borderie et al., Phys. Rev. Lett. **86** (2001) 3252
- [16] H.Feldmeier, K.Bieler, J.Schnack, Nucl. Phys **A586** (1995) 493
- [17] A.Ono, Phys. Rev. **C59** (1999) 853
- [18] A.Onishi and J.Randrup, Phys. Lett. **B394** (1997) 260
- [19] V.Baran et al., Nucl. Phys. **A703** (2002) 603
- [20] S.Ayik, C.Gregoire, Phys. Lett. **B212** (1998) 269
- [21] J.Randrup and B.Remaud, Nucl. Phys. **A514** (1990) 339
- [22] G.F.Burgio, Ph.Chomaz, J.Randrup, Phys. Rev. Lett. **69** (1991) 885
- [23] S.Ayik, E.Suraud, M.Belkacem, D.Boilley, Nucl. Phys. **A545** (1992) 35c
- [24] J.Randrup and S.Ayik, Nucl. Phys. **A572** (1994) 489
- [25] D.Durand, Nucl.Phys. **A541** (1992) 266
- [26] J.Frankland et al., Nucl. Phys. **A689** (2001) 940
- [27] M.Colonna, Ph.Chomaz, S.Ayik, Phys.Rev.Lett. **88** (2002) 122701
- [28] G.Batko and J.Randrup, Nucl. Phys. **A563** (1993) 97
- [29] H.S.Xu et al., Phys, Rev. **C48** (1993) 933; W.Bauer, G.F.Bertsch and H.Schultz, Phys. Rev. Lett **69** (1992) 1888; B.Borderie et al., Phys. Lett. **B302** (1993) 15
- [30] S. Hudan et al., (INDRA collaboration), Phys.Rev. **C67** (2003) 064613
- [31] M.Colonna, J.Cugnon and E.C.Pollacco, Phys. Rev. **C55** (1997) 1404
- [32] V.K.Rodionov et al., Nucl. Phys. **A700** (2002) 457
- [33] N.Le Neindre, Ph.D. Thesis, University of Caen, France, 1999, LPCC-T-9902; B.Borderie et al., arXiv:nucl-ex/0311016